Study the ductility of lap joints in reinforced concrete beam to propose more sustainable design

Mosleh Tohidi*[1], Yakubu Mustapha[1a], Ali B-Jahromi[1b] , and Alan Janbey[2a]

[1] School of Computing and Engineering, University of West London, St Mary's Rd, London W5 5RF, UK
[2]Engineering Department, London College UCK, 680 Bath Rd, Cranford, London, TW5 9QX , UK

(Received , Revised , Accepted)

Abstract : The Fib Model Code 2010 established new design criteria for tension laps, which are expected to influence the forthcoming version of Eurocode 2 scheduled for release in 2023. In contrast to earlier Eurocode 2 standards, the Model Code 2010 advocates for extended lap lengths, which may lead to longer lap joints when compared to the British Code (BS 8110-1). This research seeks to improve the sustainability of reinforced concrete (RC) frame structures by investigating the implementation of shorter lap lengths to decrease steel usage in concrete constructions, thereby reducing CO2 emissions. A thorough examination, incorporating both experimental and numerical methods, was performed to evaluate the effects of rebar lap joints on the strength and ductility of beams. The experimental component concentrated on simply supported reinforced concrete beams featuring lap splices subjected to four-point bending, with variations in lap lengths and two types of reinforcement bars. The results demonstrated that an increase in lap splice length contributes to enhanced stiffness, resistance, and ductility of the beams.The findings revealed that increasing the lap splices beyond 50Ø did not provide any further advantages regarding strength and ductility. Therefore, it can be inferred that the existing Eurocode 2 guideline for lap length (62Ø) is not justifiable. This enhancement results in lower labor costs and a reduced installation duration, thereby contributing to a substantial decrease in CO2 emissions.

Keywords: CO2 emissions, Sustainability, Lap joints; tension lap; development length; ductility; strength, bond.

1. Introduction

Lap splices of reinforcing bars are frequently employed in the construction sector to address the requirements of construction joints, the constraints associated with bar lengths, and the application of shorter bars. Typically, steel manufacturers provide reinforcing bars in lengths varying from 6 meters to 18 meters; however, utilizing bars of different lengths is often more practical on-site, thereby necessitating the regular implementation of lap splices.

In concrete constructions, reinforcing bars are vital for enduring stress. The interaction between the steel and concrete enables effective stress transfer from the bars to the surrounding concrete. To guarantee reliable stress transmission, it is imperative to implement sufficient lap splices. The term lap splice length, or lap length, denotes the length of reinforcing bars that are interconnected with another bar. In contrast, the length of reinforcing bars that remain unconnected to another bar is termed the development length.

Concrete structures are developed based on a variety of globally recognized principles. Nonetheless, recent investigations have indicated that national and international codes present differing requirements regarding lap and anchorage lengths. For instance, the Fib Model Code for Concrete Structures (2010) and BS EN 1992-1-1 (2004) provide distinct formulations for determining lap length. The equations in BS EN 1992-1-1 (2004) are derived from CIBFIP (1991), whereas the Fib Bulletin (2013) utilizes a regression analysis as described in TG4.5 (2014). The design equation for average lap stress presented in Fib Bulletin 72 (2014) was calibrated using a lap database created by the Institute of Construction Material and the American Concrete Institute at the University of Stuttgart, and it was further validated through anchorage tests performed by Amin (2009). Despite comprehensive research into the factors influencing lap lengths, the design models for lap lengths in the latest draft of Eurocode 2 and Fib Bulletin (2013) do not possess a robust foundation for establishing design values.

Research by Cairns and Eligehausen (2014) indicates that the safety margin associated with the proposed lap length in Eurocode 2 (BS EN 1992-1-1, 2004) is less robust than anticipated. Although earlier national standards prescribed

*Corresponding author, Ph.D. Post-doc research fellow
E-mail: mosleh.tohidi@uwl.ac.uk
[a]Ph.D.
[b]Professor

doi: 10.1006/efs.xxxx.xxxx ISSN: 2753-4693

shorter lap lengths, there have been no significant instances of lap failures reported to date. Nevertheless, designers in the UK express concerns regarding the extension of lap lengths, as the reinforcement detailing outlined in the current Eurocode 2 is already considered unsustainable due to factors such as project costs and construction complexity. To enhance the ductility of beams, Eurocode 2 advocates for the staggering of lap splices. Recent investigations have cast doubt on the relevance of α_6 (the percentage of bars lapped at a given location) as specified in clause 8.7.3 of Eurocode 2, positing that the proportion of lapped reinforcement has a negligible effect on resistance, while it significantly influences deformation capacity and residual strength (Cairns and Eligehausen, 2014).

Designers are presented with three alternatives for tension laps in accordance with Eurocode 2: (a) offsetting the laps to enhance residual strength, (b) incorporating confinement reinforcement to augment deformation capacity, and (c) designing the lap to withstand $1.2\sigma_{sd}$, thereby ensuring that brittle failures manifest only after significant plastic deformations occur beyond the lap length. In cases where the staggered lapped bars constitute 35% or less of the total cross-sectional area of the reinforcing steel in linear structural elements such as beams and columns, tension laps can be designed for σ_{sd},.

Cairns (2013, 2014) posits that staggered laps may lead to a weakening effect, as the strain experienced at the loaded end of lapped bars is significantly greater than that of the neighboring continuous bars. Furthermore, it is essential that the total elongation of both continuous and lapped bars remains consistent.

To achieve adequate spacing for lapped reinforcement bars, the ACI Committee 318 -2011 (2011) advises that the splice length should be extended to 1.3 times the anchorage length when more than 50% of the bars are overlapped. In contrast, Eurocode 2 adopts a more cautious stance, suggesting that the splice length may need to be increased to as much as 1.5 times the anchorage length, depending on the proportion of bars that are spliced at that particular location. Furthermore, the Fib Model Code (2010) stipulates that if all bars are spliced at a single section, the lap length could be required to reach up to twice the standard anchorage length.

The capacity of the Earth to support life has reached a pivotal juncture, resulting in irreversible harm to the planet, its resources, inhabitants, and ecosystems (Uher and Lawson, 1998; Ortiz, Castells and Sonnemann, 2009; Yılmaz and Bakış, 2015). As a result, sustainability has become a critical global issue, prompting the introduction of significant measures to address urgent challenges such as the depletion of natural resources, air pollution, climate change, waste production, and environmental degradation in urban areas. To effectively confront these issues, it is essential to achieve a reduction of approximately 50% in emissions by the year 2050, given that environmental crises such as global warming and climate change are largely driven by carbon dioxide (CO2) emissions and other greenhouse gases that are already affecting human populations (Yılmaz and Bakış, 2015).

The construction sector plays a crucial role in delivering vital infrastructure and buildings that support both societal needs and economic development. However, it is also a major contributor to carbon dioxide emissions, primarily due to the manufacturing processes of materials such as cement and steel, as well as the greenhouse gases emitted during construction operations and the waste produced from renovation and demolition activities (González and García Navarro, 2006; Malhotra, 2010).

The necessity for immediate intervention to avert the exhaustion of the Earth's limited natural resources has been underscored. Professionals in the construction field across the globe are increasingly focused on enhancing building practices to alleviate negative environmental effects. In support of this worldwide movement, the UK Building Leadership Council, in conjunction with the UK Government, launched the Construction Industry Deal in July 2018, which allocated £420 million to facilitate the transformation of the industry. Although numerous facets of the construction sector require consideration, it is essential to prioritize sustainability in the design of various components of reinforced concrete (RC) structures to minimize the consumption of cement, steel, and aggregate during the construction process.

1.1 Current design model for lap lengths

Structural design codes for members include design models that consider stress in bonding areas. These models are regularly revised with each new edition of the code. The team responsible for Eurocode 2 has introduced a new proposal for the next iteration of Eurocode 2. The lap design model is based on Fib Bulletin 72, which acts as the foundational document for Model Code 2010. Furthermore, the Eurocode 2 project team has offered initial calibration factors to transition from the average values presented in Fib Bulletin 72 to design values, which are still pending verification for lap design models.

Different design codes present unique specifications regarding lap lengths in models that either include or exclude bond strength definitions. Historically, Model Code 2010 and Eurocode 2 established lap lengths contingent upon bond strength across various concrete classes. In contrast, the ACI and Fib Bulletin models were formulated through statistical evaluations of experimental data, focusing on the maximum bar strength in laps rather than assessing bond strength. It is important to highlight that the bond strength for Model Code 2010 was derived from the Fib Bulletin 72 design model.

The design model outlined in Eurocode 2 offers a systematic approach for calculating the necessary lap length of reinforcing bars within concrete structures. This model incorporates various factors, including tensile strength, the positioning of bars, and their diameters, to ascertain the design bond strength, anchorage length, and lap length. The calculation of anchorage length involves several parameters, such as the shape of the bars, the concrete cover, the shear link ratio, and the transverse pressure. Eurocode 2 advises that laps should be situated in regions of low moment, staggered appropriately, and that the clear spacing between lapped bars should not exceed 50 mm or 4∅. In instances where all bars are arranged in a single layer, the allowable percentage of lapped bars under tension is 100%, while for

doi: 10.1006/efs.xxxx.xxxx ISSN: 2753-4693

multiple layers, this percentage should not surpass 50%. Additionally, shear links are required to be positioned at the outer section of the lap length to effectively concentrate the splitting forces at the ends of the lap, as specified by Eurocode 2. If the proportion of lapped bars is below 25%, it may be assumed that shear links are adequate for other considerations.

Orangun et al. (1977) developed a design model that continues to be utilized in the ACI Code of 2011. The initial step in calculating the lap length is to ascertain the anchorage length. This process requires consideration of several factors, such as compressive strength, concrete cover, bar diameter, bond conditions, and the shear link ratio. A confinement ratio greater than 2.5 indicates a heightened risk of pull-out failure.

In research carried out by Tohidi (2017), a series of 65 pull-out tests were performed on different reinforcement bar diameters (8 mm, 10 mm, 12 mm, and 16 mm) within the keyways of precast slabs. The results of this investigation led to the formulation of a proposed model for development length, which indicated a safety factor of 1.3 in relation to the EC2 model for both development and lap lengths.

According to Fib Bulletin 72, the working draft from PTI proposes an updated design model for the next version of Eurocode 2. This model indicates that lap splices should be designed to accommodate 1.2 times the specified development length.

Micallef and Vollum (2018) observed that samples with longer splice lengths exhibited reduced splitting along their length, whereas shorter splices experienced significant splitting over a considerable portion. In a different investigation, Najafgholipour et al. (2018) analyzed the behavior of lap splices in reinforced concrete (RC) beams, utilizing two distinct bar diameters (12 mm and 16 mm) under cyclic loading conditions. This study emphasized factors such as transverse reinforcement, splice length, and the grade of longitudinal steel bars. The findings indicated that beams adhering to ACI lap splice length criteria displayed questionable performance when subjected to cyclic loads. Conversely, beams with a 25% increase in lap length demonstrated sufficient flexural ductility and were able to withstand cyclic loading effectively.

1.2 Issues with lap joint detailing

In the analysis of bond behavior, it is crucial to recognize that the samples employed for calibrating coefficients in experimental settings may not truly represent standard construction methodologies. Several significant distinctions between the two are as follows:

1. In experimental settings, lapped or spliced joints are frequently situated in the regions of a sample that experience the highest levels of stress. Conversely, in practical applications, designers generally opt to position these joints in areas where the stress from reinforcement is minimal.

2. During experiments, lap joints or splices are commonly located in the constant moment zone of a beam, where the shear force is effectively zero. In contrast, practical applications typically involve placing these joints in regions where shear forces are active.

3. In most experimental scenarios, the lapped bars are of uniform diameter; however, in real-world applications, variations in diameter between the bars are often observed.

A research investigation was carried out by Reynolds and Beeby (1982) to evaluate the strength of shear span laps in comparison to equivalent laps situated in regions of constant moment. The findings indicated that the shear span laps exhibited greater strength, which the researchers ascribed to the heightened stress experienced by the transverse reinforcements.

The bond model within the region of fluctuating moments was assessed through development-length experiments carried out in the United States during the 1960s and 1970s. Jirsa et al. (1995) recognized the difficulties associated with performing bond experiments under shear conditions; however, they observed no significant difference in bond strength when shear and moment were applied concurrently in a single bond failure test. These results are consistent with the findings of Vollum and Micallef (2018), who similarly determined that shear does not influence the bond strength of the tested laps. Although definitive evidence is lacking, it has been suggested that variations in force at the ends of the laps may enhance the average bond strength.

Under typical service conditions, a bar lap splice situated at the point of contraflexure will encounter stresses that approach the design strength of the reinforcing bar, yet remain considerably below its ultimate yield strength. Conversely, if an internal column is eliminated as a result of unusual loading conditions, the beam will be required to span in two directions rather than one, leading to considerable deflections. The primary load-bearing mechanism will transition from flexural action to catenary action, contingent upon the support conditions.

To avert total failure, it may be essential for the lap joint to experience strains that exceed the yield point. Furthermore, it is recommended that the connections designed to resist significant collapse possess the capacity to yield, rather than failing in a potentially brittle fashion as a result of bond failure.

The lap length necessary to attain the design strength of a reinforcement bar can be considerably diminished under the provisions of Model Code 90, allowing for a reduction to merely 30% of the initial length. This significant decrease is achievable when the reinforcement area supplied is three times greater than the minimum requirement. Furthermore, in scenarios where the provided area is double the required amount and only 20% of the bars are spliced at a specific location, Model Code 90 allows for a lap length of 30% of the total design length. Nevertheless, the authors advocate for the use of a full lap length in structures engineered to resist progressive collapse (Tohidi, 2017).

Research has surprisingly revealed a lack of scholarly attention towards the percentage lapped parameter, despite its considerable influence on bond length. In a study by Magnusson (2000), four distinct tests were performed in which only a segment of the reinforcement was spliced at designated locations. The findings indicated that an increase in the proportion of continuous reinforcement corresponded with marked enhancements in flexural strength. Specifically, experiments in which only half or one-third of the bars were

doi: 10.1006/efs.xxxx.xxxx ISSN: 2753-4693

spliced exhibited strengths that were 50% and 100% greater, respectively, than the control samples in which all bars were spliced.

Ferguson and Briceno (1965) performed a comparative analysis of three beams, each featuring splices at identical sections, alongside four analogous samples in which 50% of the bars remained continuous throughout the lap region. The samples characterized by 50% spliced bars demonstrated an average strength increase of 10 to 15%.

Chinn et al. (1955) and Vollum and Micallef (2018) arrived at similar conclusions regarding the application of continuous edge bars in certain samples while employing spliced bars in others for the process of wide beam lapping. Their investigations revealed that shear forces did not significantly influence the strength of the lap joints examined. Furthermore, increasing the lap lengths beyond the necessary threshold for achieving reinforcement yield did not enhance ductility.

Previous investigations, as outlined in the earlier section, have largely focused on evaluating the effects of bond strength, transverse reinforcement, bar diameter of lap joints, and lap length at a single-lap location (Rezansoff and Fu, 1992; Einea and Tadros, 1999). These studies have mainly utilized four-point bending tests on beams featuring lap splices located within the constant moment zone. However, a design model for concrete structures that incorporates lapped stainless-steel reinforcement is currently lacking. Furthermore, the author has noted a deficiency in experimental research aimed at establishing the minimum lap length required for rebar rotation to occur before the formation of a plastic hinge in reinforced concrete beams. This consideration is crucial for the evaluation of structural integrity and the application of performance-based design methodologies.

An experimental investigation involving four columns revealed that the placement of lap splices within the columns has a significant impact on both strength and ductility. The findings indicated that the column with lap splices situated in its critical region exhibited the highest strength, albeit with the lowest ductility performance. Conversely, the column with lap splices positioned outside the critical region demonstrated strength and ductility levels similar to those of a column devoid of lap splices. In light of these findings, a recommendation is made regarding the optimal positioning of longitudinal steel lap splices in reinforced concrete columns (Pam and Ho, 2016).

According to a experimental study on a typical RC frame indicated that, modifying the lap splices of structural components to allow for enhanced flexibility improves both constructability and productivity. This improvement leads to a decrease in labor expenses and a shorter installation time, ultimately facilitating a significant reduction in costs related to CO2 emissions (Daniel et. al., 2023).

1.3 Structural Application of Stainless Steel

Stainless steel is extensively utilized in structural engineering owing to its remarkable resistance to corrosion. It exhibits advantageous properties such as excellent formability, recyclability, and outstanding mechanical characteristics (Shamass, 2019). Furthermore, stainless steel boasts a prolonged lifespan and necessitates minimal upkeep. When compared to mild steel, it demonstrates enhanced strain-hardening capacity and ductility, rendering it an optimal selection for ductile sections that act as early warning systems for potential structural failures. The application of stainless steel in construction can be traced back to the 1920s, where it was primarily employed for façade and roofing applications (Baddoo, 2008). In recent times, there has been a notable increase in the use of stainless steel for load-bearing applications that require strength, ductility, durability, stiffness, and high resistance. This material is available in various forms, including tubes, plates, sheets, bars, fasteners, fixings, as well as rolled and cold-formed structural sections. Among these, cold-formed sections made from steel plates are the most prevalent materials for structural components, attributed to their broad availability and ease of manufacturing (Gardner, 2005).

Reinforced concrete serves as a prevalent structural solution within the domain of building construction. Its widespread adoption can be attributed to its efficiency, economic viability, and adaptability, as it meets a variety of performance standards and design specifications. Recently, the incorporation of stainless steel into reinforced concrete frameworks has proven advantageous, owing to its outstanding ductility, considerable strain hardening, superior durability, remarkable resistance to corrosion, and extended lifespan. Additionally, the effective use of readily available constituent materials enhances the broad application of reinforced concrete in diverse structures, such as bridges, high-rise buildings, and tunnels.

The mechanical properties of stainless steel are markedly distinct from those of carbon steel. Stainless steel displays a smooth and continuous response from the outset, characterized by high ductility and pronounced strain hardening, lacking a distinct yield point. In contrast, carbon steel exhibits a more linear behavior during the elastic phase, featuring a moderate level of strain hardening and a clearly identifiable yield point. In instances where the yield point is not easily discernible, the 0.2% proof stress is typically utilized in design applications. The characterization of stainless steels is frequently conducted using the modified-good stainless steel material model, which represents an advancement of the original framework proposed by Rasmussen (2003).

Stainless steel reinforcement demonstrates enhanced mechanical properties, including increased hardness and strength, when compared to conventional carbon steel (Gonzalez et al., 2003). Medina et al. (2015) conducted an analysis of the mechanical and ductility characteristics of stainless steel grades 1.4482, 1.4301, and 1.4362, juxtaposing them with carbon steel grade B500SD. Their findings indicated that stainless steels exhibit ductility levels that are three times greater than those of carbon steel. Nevertheless, it was noted that the elasticity modulus of these stainless steels is approximately 15% lower than that of carbon steels. This difference can be explained by the nonlinear behavior of stainless steels observed from the early stages, which complicates the precise measurement of the modulus of elasticity.

The durability of carbon steel reinforcement in reinforced

concrete structures is often not as reliable as previously anticipated under various conditions (British Stainless-steel Association, 2003). In particularly aggressive environments, such as coastal and marine areas, the corrosion of carbon steel can lead to significant and costly rehabilitation efforts. In these contexts, stainless steel reinforcement emerges as a highly effective and durable alternative. A notable case is the Gatwick bridge in Australia, constructed in 1986 with grade stainless steel, which exemplifies the successful application of stainless-steel reinforcement. Impressively, this bridge has remained operational for over 70 years without requiring substantial maintenance or major repairs.

The Saint George Bridge located in Genoa and the AIIt Chonoglias Bridge in Scotland serve as notable instances of infrastructure projects that have integrated stainless steel reinforcement. Both bridges have been built employing stainless steel materials. The application of stainless steel reinforcement extends beyond new constructions, encompassing restoration and renovation efforts as well.

2. Significance of the research

Following the conclusion of the Second World War, the swift economic advancements in the construction sector, coupled with a significant demand in urban regions, have led to the detrimental over-extraction of natural resources, including fossil fuels, minerals, forests, and land. In response to pressing global challenges such as the consumption of natural resources, air pollution, climate change, waste generation, and environmental degradation in major urban centers, a series of radical reforms have been suggested over the past decade. In accordance with this strategic initiative, the integration of sustainability into construction practices has emerged as a paramount concern in the design of all projects.

The importance of this research lies in its aim to decrease the consumption of reinforcement bars, thereby reducing CO2 emissions in reinforced concrete structures. This is achieved through the proposal of a more optimized and sustainable lap length in concrete beams.

This research is distinguished by its examination of how rebar laps influence the ductility of reinforced concrete (RC) beams, alongside the identification of the minimum lap length required for rebar rotation before the formation of the plastic hinge.

3. EXPERIMENTAL STUDY

This study focuses on the potential for minimizing lap lengths and, consequently, reducing CO2 emissions, while ensuring that the performance of reinforced concrete (RC) elements remains uncompromised. To do so, the strength and ductility of concrete beams using different lap lengths considerting both carbon steel and stainless steel have been investigated. The properties of concrete and rebars assumed to be constant.

3.1 Material properties

Concrete

To exemplify the concrete typically utilized in industrial settings, a target compressive strength of 30 MPa was established. The workability of the concrete was evaluated via the slump test, conducted with the 'ELE International Slump Test Kit BS and ASTM 34-0192'. Subsequently, the compressive strength of the specimens was measured using the ELE ADR-Auto V2.0 2000 standard (see Fig. 1a). The assessment of compressive strength was performed using a compression machine operating at a velocity of 10.6 m/s (refer to Fig. 1b).

Reinforcement (Carbon Steel)

The testing program employed mild reinforcing bars with diameters of 8 mm and 12 mm, conforming to the specifications outlined in BS EN 1992-1-1 (2004). These bars were procured from a local supplier, Metal4U. Initially, the reinforcing steel bars were delivered in lengths of 6 m and were subsequently cut into various sizes within the laboratory environment. Special attention was given to ensure that any damaged bars were excluded from the lapped sections of the beam specimens. The steel utilized in the experiments remained in its original condition as received, without any surface treatment or specialized cleaning. In contrast, the link cages were fabricated using an 8 mm diameter reinforcing bar drawn from the laboratory's existing inventory.

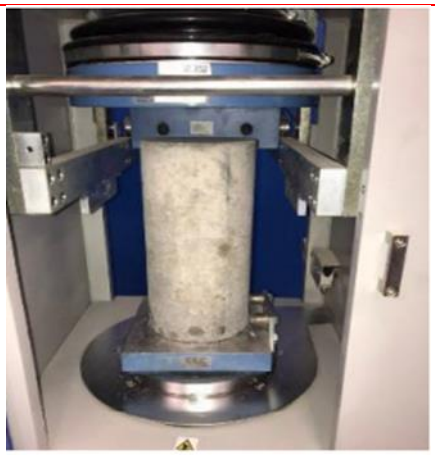

(a) Compressive strength test

(b) ELE ADR-Auto V2.0 2000 Standard

Fig. 1 Compressive strength apparatus

doi: 10.1006/efs.xxxx.xxxx

ISSN: 2753-4693

The Instron 5584, a 150 kN electromagnetic frame, serves as the equipment utilized for evaluating the tensile strength of reinforcing bars. This apparatus is complemented by an Instron 2640 extensometer, which features a gauge length of 50 mm. The results from the experimental analysis performed on 12 mm reinforcing bars are illustrated in Figure 2.

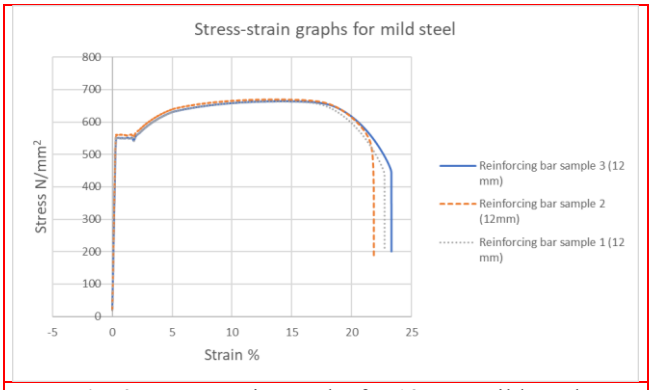

Fig. 2 Stress-strain graphs for 12 mm mild steel reinforcement.

3.1 Geometry and properties of test specimens

Flexural test (beams without reinforcement)

Figure 3 depicts the distinct features of the specimens along with the loading methodology employed. Following the standards set forth in BS EN 12390-5:2020, the dimensions of the plain concrete beam specimens were established at 150 mm × 150 mm × 750 mm (see Fig. 3). A compression machine was utilized to apply a crushing force to the three beam specimens at a rate of 0.45 kN/s.

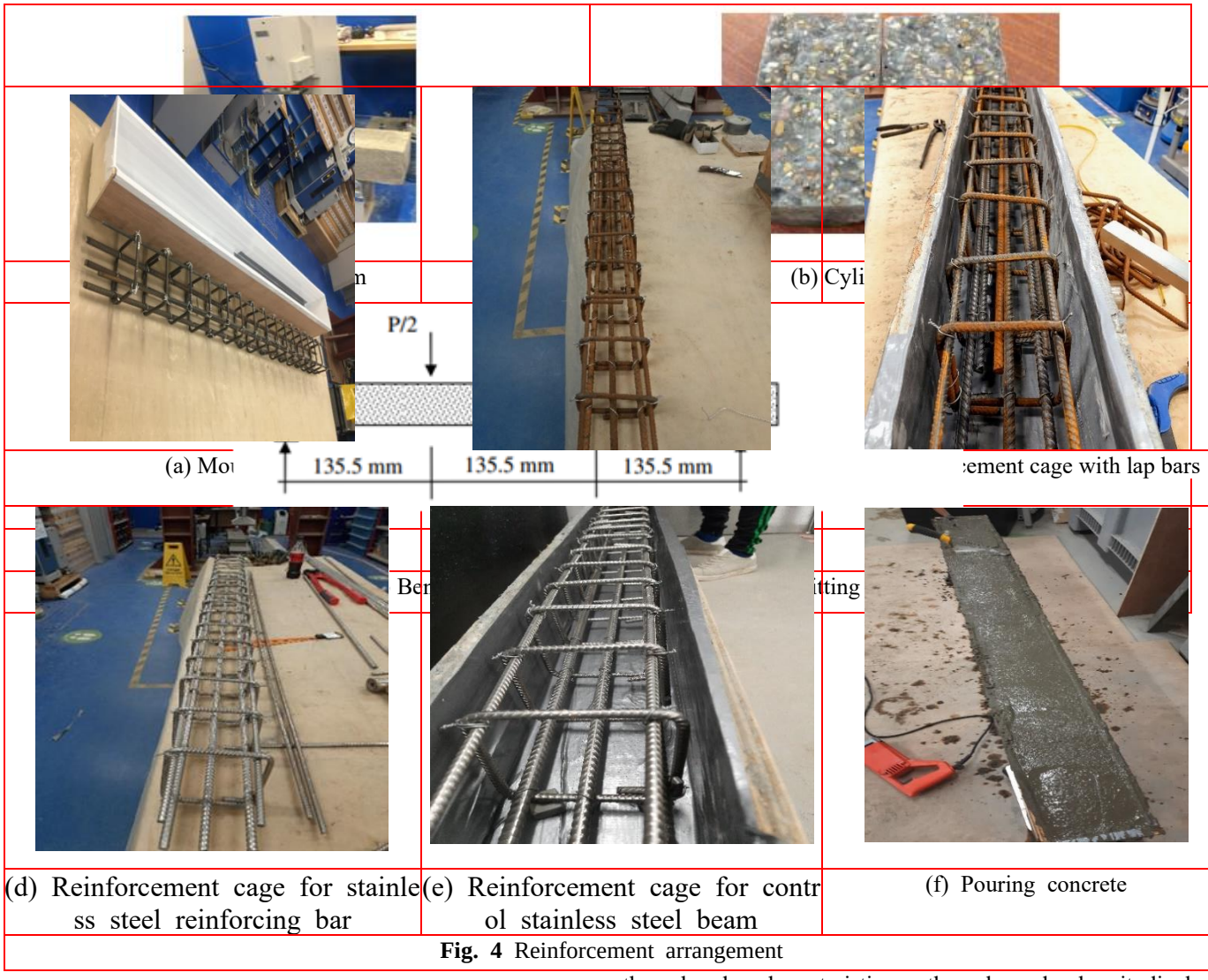

(a) Mo… (b) Cyli… …cement cage with lap bars

(d) Reinforcement cage for stainless steel reinforcing bar (e) Reinforcement cage for control stainless steel beam (f) Pouring concrete

Fig. 4 Reinforcement arrangement

Flexural test (reinforced concrete beam)

Upon the conclusion of the slump test, individual beams were fabricated utilizing marine plywood for the formwork (see Fig. 4a). During the casting phase, the tension reinforcement bars were arranged horizontally. To maintain stability, the reinforcement cage was carefully placed within the mold and secured with a 15 mm concrete cover that was affixed to both the sides and the base of the cage. To improve the bond characteristics, the lapped longitudinal reinforcement was strategically located at the bottom of the formwork in the lap test specimens. The concrete was introduced in two distinct layers and was compacted with the aid of a mechanical vibrator poker. Ultimately, the upper

(a) Test specimens

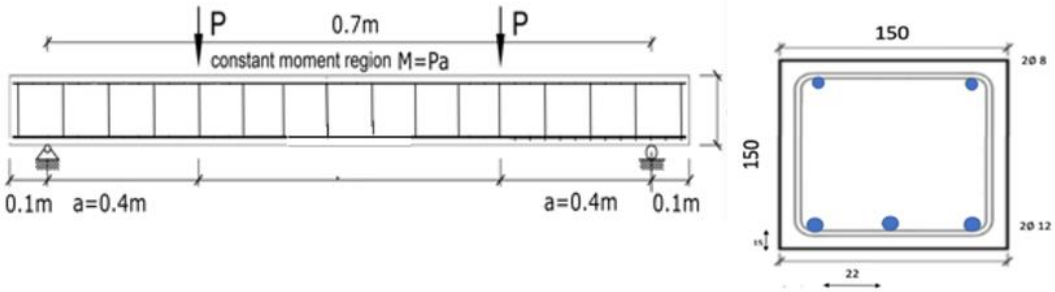

(b) Geometry and typical reinforcement arrangement of the experiments

Fig. 5 Experimental set-up with linear variable displacement in position

surface of the beams was finished with a stainless-steel float, yielding a polished appearance, as illustrated in Fig. 4f.

The primary beams were produced concurrently with three cylindrical samples, each measuring 150 × 300 mm, alongside three cubic specimens of dimensions 150 × 150 × 150 mm. All samples were fabricated from the same batch of fresh concrete. The objective of creating both the cube and cylinder samples was to evaluate the compressive and tensile strength of the concrete. After the casting procedure, all cubes and cylinders remained in their molds for a period of twenty-four hours.

Following this, the formwork for the cubes and the molds for the cylinders were dismantled. The samples were subsequently placed in a curing tank maintained at a temperature of (20 ± 2) °C until the testing phase, which took place after a duration of 28 days.

3.2 Test Setup and Instrumentation

The specimens for the primary reinforced concrete beams were situated centrally within the hydraulic actuator, with a vertical load exerted on the upper central surface of the beam (see Figure 5). These beams were subjected to four-point bending, featuring a span of 700 mm and a shear span of 400 mm. The intervals between the two loading points were strategically located within the constant moment region (see Figure 5). It is noteworthy that the selected termination criteria for the hydraulic actuator during the experimental setup was based on deflection control. This approach was adopted to establish a threshold related to deflection throughout the testing process, as it was more feasible and served to mitigate potential damage to the variable displacement transducer positioned at the beam's base. As a result, the actuator was programmed to conclude the experiments when the midspan deflection of the beam reached 100 mm or upon the occurrence of splice failure, whichever event transpired first.

A hydraulic actuator was utilized in this research, characterized by a stroke length of 350 mm and a maximum load capacity of 500 kN. The initial displacement rate was measured at 0.2 mm/min; however, this rate increased following the yielding of the rebar or upon reaching the peak load. To facilitate the application of the load, a machine ramp was employed, and a rigid steel beam measuring 150 mm × 150 mm × 750 mm was centrally positioned on the reinforced concrete (RC) beam specimen. This configuration allowed for a uniform distribution of the load across two point loads (P1 and P2), which were spaced 0.7 m apart on the beam. The hydraulic actuator's ability to apply the necessary ramp load and to record the corresponding deflection at the midspan of the beam is depicted in Figure 5. This capability was enabled by a built-in AEP TC4 transducer, with the data being recorded using LabVIEW-based software linked to the actuator. Additionally, a variable displacement transducer was installed at the center of the bottom face of the beam, complementing the built-in displacement transducer.

3.3 Geometry and properties of test specimens

This study investigates three stainless steel beams alongside five reinforced concrete beams, each incorporating mild steel reinforcing bars for the experimental procedures. The splicing of the beams occurred at the region of maximum moment, with the exception of the control beams, which

doi: 10.1006/efs.xxxx.xxxx ISSN: 2753-4693

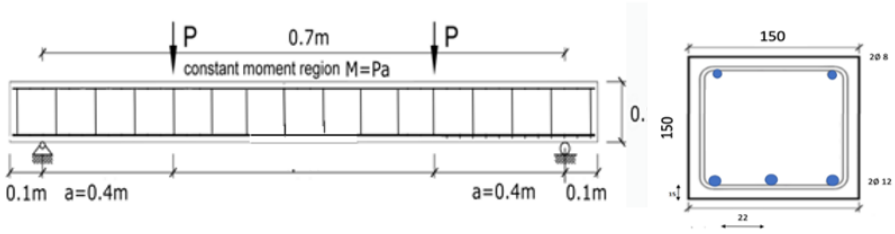

(a) Control

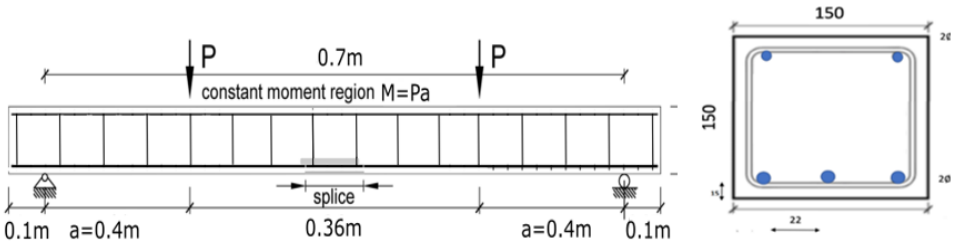

(b) Lap length= 30Ø (360 mm)

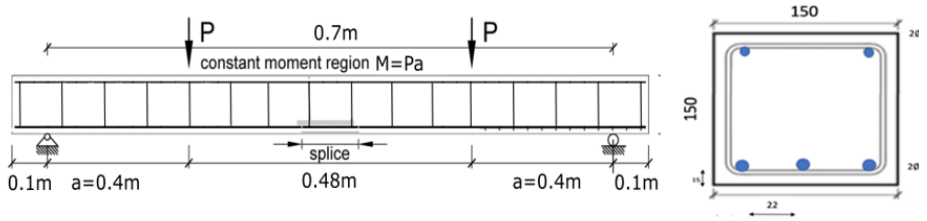

(c) Lap length= 40Ø (480 mm)

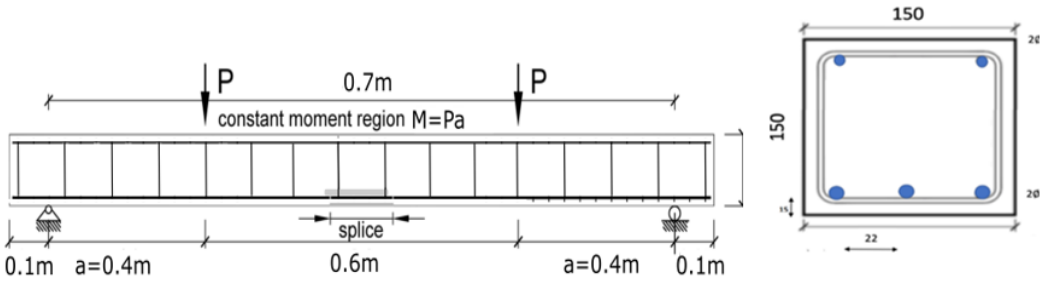

(d) Lap length= 50Ø (600 mm)

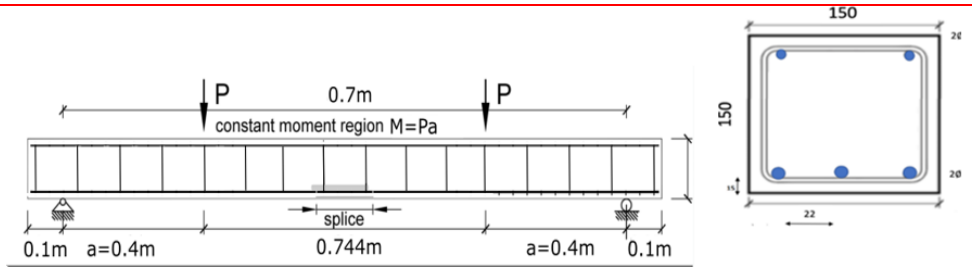

(e) Lap length (EC2)= 62Ø (744 mm)

Fig. 6 Details of reinforcement and geometry of designed experiments

functioned as a baseline reference. The lengths of the splices analyzed in this research are 30Ø, 40Ø, 50Ø, and 62Ø. For a visual depiction of the reinforcement and geometry of these beams, please consult Figure 6.

doi: 10.1006/efs.xxxx.xxxx
ISSN: 2753-4693

Table 1. Material properties of reinforced concrete beams

Beam	Concrete			Reinforcement				
	Young's modulus E (N/mm^2)	Compressive strength f_{ck} (N/mm^2)		Diameter (d) (mm)	Material	Yield stress f_y (N/mm^2)	Tensile strength (R_m) (N/mm^2)	Young's modulus MPa
Control	28E3	32		12	Carbon Steel	559.91	664.05	210E3
30Ø lap	28E3	32		12	Carbon steel	559.91	664.05	210E3
40Ø lap	28E3	32		12	Carbon steel	559.91	664.05	210E3
50Ø lap	28E3	32		12	Carbon steel	559.91	664.05	210E3
EC2 (62Ø)	28E3	32		12	Carbon steel	559.91	664.05	210E3

Table 2 Mean compressive of the cylinders

ID	Compressive strength MPa	Average compressive strength
SP 1	32.61	32.72
SP2	32.67	
SP3	32.87	

All beams underwent testing under monotonic loading conditions, specifically through four-point bending, utilizing continuous displacement control until failure occurred. The reinforcement characteristics for each beam, along with the material properties of the concrete, are detailed in Table 1. The tensile strength and elastic modulus of the specimens were determined through the conducted tests.

3.4 Stainless steel

The enhanced strain hardening and ductility of stainless steel, in contrast to mild steel, presents a notable advantage. This property, coupled with its ductility, has resulted in many international design codes, including Eurocode 2, not providing a distinct design model for concrete structures that utilize stainless steel reinforcing bars. The background documentation for Eurocode 2 indicates that there are no technical barriers to applying the Eurocode 2 design framework alongside other reinforcement types, provided that their specific properties and behaviors are duly considered. However, this assertion holds true primarily for mild steel reinforcing bars, as it can yield erroneous outcomes when a stainless steel reinforcing bar with a lap splice is utilized in a reinforced concrete configuration. Although numerous studies have been conducted on the performance of structures incorporating stainless steel in recent years, the majority of this research has concentrated on plain stainless steel components rather than on reinforced concrete or stainless steel reinforced concrete featuring lap splices. Therefore, the aim of this section is to evaluate and compare the performance of stainless steel and mild steel reinforced concrete, considering both scenarios with and without lap splices.

Material characteristics

Concrete

To attain a target concrete compressive strength of C30, specific mix proportions were utilized. These proportions included a water-to-cement ratio of 0.45, along with 21 kg of cement, 52.50 kg of fine sand, and 23.39 kg of coarse aggregate. The maximum aggregate size incorporated in the mixture was 10 mm. For the flexural testing of the beams, three beam specimens, each measuring 150 mm × 150 mm × 750 mm, were cast from the same batch. This approach ensured uniformity in the testing procedure and adhered to the standards set forth in BS EN 12390-5(2020).

Furthermore, three cylindrical samples of concrete were produced using the identical concrete mixture. These samples were utilized to determine the compressive strength of the concrete. The testing for compressive strength was conducted in compliance with the standards set forth in EN12390-3 (2009).

Following the casting of the concrete, the cylinders and beams were transferred to a curing tank after a period of 24 hours. This procedure facilitated the adequate curing and enhancement of the concrete specimens. The average compressive strength of the concrete for the three cylinder samples is presented in Table 2.

Stainless steel rebar property

The EN 1.4301 grade 304 stainless steel, recognized as the most commonly utilized grade, is distinguished by its exceptional corrosion resistance, specific composition, and favorable mechanical properties (Metals4u, 2021). In this investigation, grade 304 stainless steel was selected due to its ready availability from local suppliers and its widespread application across various sectors. Two distinct diameters of stainless steel reinforcing bars, specifically 8 mm and 12 mm, were employed (see Fig. 7). Both the stainless steel and mild steel reinforcing bars were designed with transverse and longitudinal ribs at each cross-section. The mild steel reinforcement conformed to the standards set forth in BS4449+A3, 2005, while the stainless steel reinforcement met the requirements of BS 6744, 2016. To assess the stress-strain constitutive behavior and mechanical properties of the stainless steel, tensile tests were performed in accordance with EN 6892-1 (2016).

doi: 10.1006/efs.xxxx.xxxx ISSN: 2753-4693

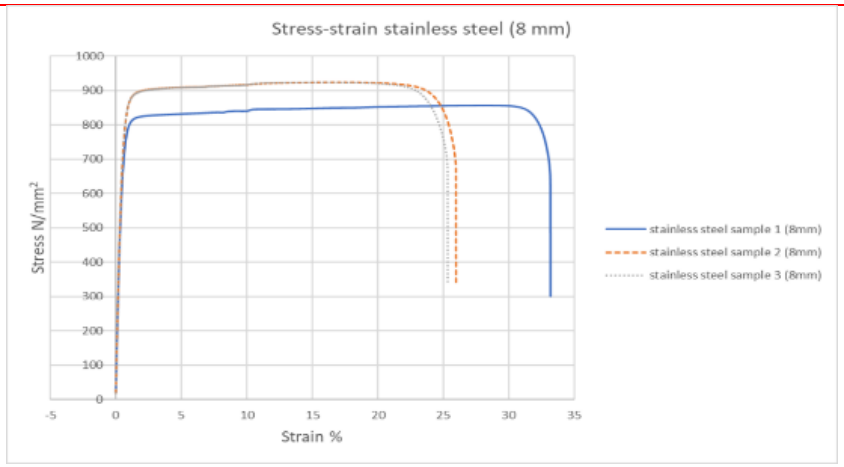

(a) 8mm

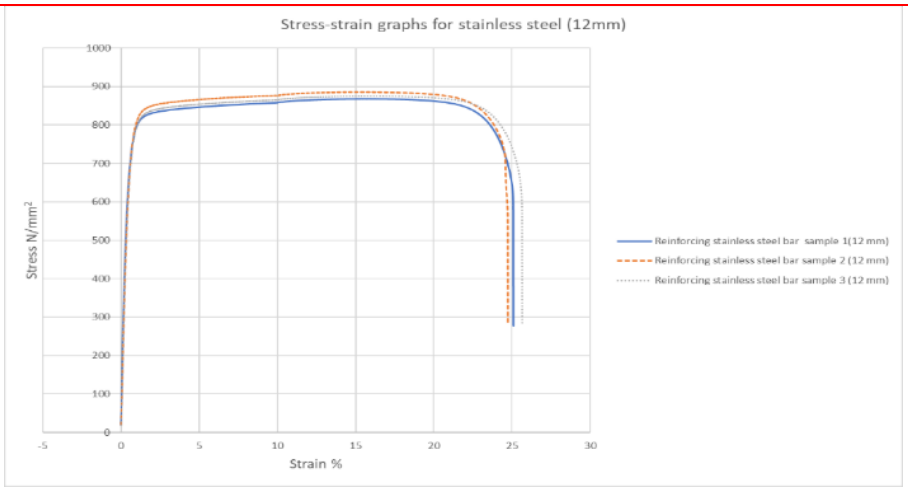

(b) 12 mm

Fig. 7 Stress-strain graphs for 8 mm and 12 mm stainless steel reinforcement

Loading set-up

A total of seven experiments were conducted on reinforced concrete (RC) beams, comprising five experiments utilizing mild steel reinforcement and two experiments employing stainless steel reinforcement. Detailed information regarding each experiment is presented in Table 1 for the mild steel specimens and Table 3 for those with stainless steel reinforcement. Among the mild steel tests, four beams (designated as MS-30Ø, MS-40Ø, MS-50Ø, and MS-62Ø) featured lap splices located at their centers, whereas one beam (SS-30Ø) with stainless steel reinforcement also included a central lap splice. The other two beams (SS-00 and MS-00) did not incorporate lap splices and were reinforced with stainless steel and mild steel, respectively.

A reference system was employed to categorize each specimen. The type of rebar was denoted by the initial two letters, where "SS" signified stainless steel and "MS" indicated mild steel. The subsequent term represented the lap splice length, with the values of 30Ø, 40Ø, 50Ø, and 62Ø corresponding to splice lengths of 360 mm, 480 mm, 600 mm, and 744 mm, respectively, as detailed in Table 4.

Figure 8(a) illustrates the arrangement of the beams, encompassing their geometric specifications and reinforcement characteristics. Furthermore, Figure 8(b) presents an image of the formwork utilized for the placement of reinforcement prior to and following the concrete casting.

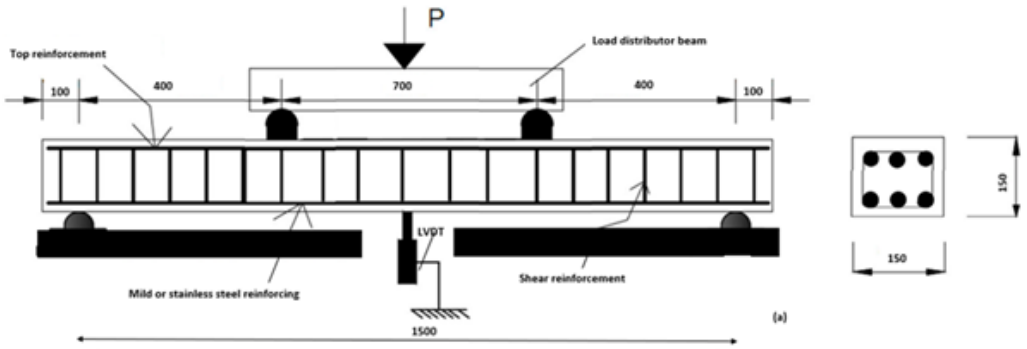

(a) The geometrical and reinforcement details

(b) Reinforcement arrangement and formwork

Fig. 8 Beam samples configuration

Table 3. Material properties of reinforced concrete beams

Beam	Concrete			Reinforcement				
	Young's modulus E (N/mm^2)	Compressive strength f_{ck} (N/mm^2)		Diameter (d) (mm)	Material	Yield stress f_y (N/mm^2)	Tensile strength (R_m) (N/mm^2)	Young's modulus
Control	177	32		12	Stainless steel	680.50	876.12	174970
30Ø lap	177	32		12	Stainless steel	680.50	876.12	174970

3.5 Experimental procedure

A hydraulic actuator with a capacity of 500 kN was utilized to exert a continuous load along the machine ramp on a load spreader beam, thereby creating two equivalent point loads on the upper surface of the beam. Throughout the experimental procedures, a displacement control technique was implemented, with a load application rate set at 0.20 mm/min. The vertical displacement at the midpoint of the beam span was recorded using an integrated TC4 transducer alongside a linear variable displacement transducer (LVDT). To capture the experimental data, software based on LabVIEW was employed, interfacing with a computer. Prior to the commencement of testing, the surfaces of all samples were thoroughly dried to enhance the visibility of crack patterns and their development.

4. Results and Discussion

4.1 Beam failure

The traditional understanding of failure in a standard reinforced concrete (RC) beam is that it occurs when the compressive strain in the outer concrete fiber exceeds the ultimate crushing strain, which is generally accepted to be around 0.0035 or 0.003. This failure mechanism is attributed to the fact that the strain at the top surface of the concrete is reached after the reinforcement has yielded, resulting in the steel no longer contributing to the beam's overall load-bearing capacity. This situation is particularly prevalent when the reinforcing material demonstrates perfectly plastic stress-strain characteristics. However, the introduction of stainless steel as a reinforcement material alters this behavior due to its enhanced ductility, strain hardening properties, and the lack of a distinct yield point. With stainless steel reinforcement, the material continues to provide support to the beam's ultimate load capacity even after the concrete at the top surface has reached its crushing strain. Additionally, accurately predicting the moment of concrete crushing poses challenges, leading to the necessity of making assumptions regarding the precise failure point. To address this uncertainty, the peak capacity of the beam is typically assessed based on the ultimate load capacity of the section, as determined through experimental methods. It is noteworthy that in this study, all samples with lap splices

experienced failure at the lap end.

Fig. 9 Control sample with mild steel

Fig. 10 Sample with the lap length of 30Ø and mild steel

Fig. 11 Sample with the lap length of 40Ø and mild steel

Fig. 12 Sample with the lap length of 50Ø and mild steel

Fig. 13 Sample according to EC2 and mild steel

During the course of the experiments, visual observations were made regarding the propagation of cracks on the tension face of the beams (see Fig. 9-13). The initial cracking occurred at a load that was approximately less than half of the ultimate failure load. In all control samples, transverse flexural cracks were first observed at the points of load application. These cracks originated at the ends of the lapped bars, subsequently leading to the development of a longitudinal crack along the edge of the lap. As the load continued to increase towards failure, the cracks extended along the laps in short and irregular segments. Notably, in beam samples with longer lap lengths (50Ø and EC2 62Ø), shear cracks propagated towards the beam support following the initial lap cracking as the load increased. The existing longitudinal cracks widened and extended across the lap length upon bond failure. The predominant failure mechanism identified in all samples featuring lap splices was bond failure. However, the beam with 30Ø laps exhibited brittle failure prior to the yielding of the steel, attributed to an inadequate lap length.

4.2 Load deflection relationships

The results of the experiments are presented in Figure 14 and Table 4. Three repetitions of experiments were performed for each type of rebar. Table 4 summarizes the average outcomes for the two reinforcement types. In this table, P_m denotes the maximum load capacity associated with the mid-span deformation (δ_m), ε_u represents the elongation at failure of the reinforcement, σ_m indicates the maximum strength of the reinforcement, l_b refers to the lap splice length, and σ_y signifies the yield strength of the rebar, which is defined as the 0.2% proof strength ($\sigma_{0.2}$) for stainless steel. The lap splice length for each beam is detailed in Table 4 through the lap length-to-bar diameter ratio (for instance, 30Ø indicates 30 times the diameter of the tension bar).

doi: 10.1006/efs.xxxx.xxxx
ISSN: 2753-4693

Table 4. The details of seven specimens and the test results

Beam	f_{ck} (N/mm^2)	l_b (mm)	σ_y (N/mm^2)	σ_m (N/mm^2)	ε_u %	P_m (KN)	δ_m (mm)	Failure mode
MS-00	32.72	N/A	554.14	665.45	22.47	77.63	15.18	[Y,c]
MS-30Ø	32.72	30Ø	554.14	665.45	22.47	64.99	12.72	[b]
MS-40Ø	32.72	40Ø	554.14	665.45	22.47	70.72	12.24	[Y,b]
MS-50Ø	32.72	50Ø	554.14	665.45	22.47	77.44	14.58	[y,b]
MS-62Ø	32.72	62Ø	554.14	665.45	22.47	88.44	12.34	[Y,b]
Eurocode 2								
SS-00	32.72	N/A	694.32	876.12	24.83	105.12	16.23	[c]
SS-30Ø	32.72	30Ø	694.32	876.12	24.83	77.29	12.57	[b,c]

Failure modes:
[b]-bond failure
[c]-crushing
[y]-yielding
δ_m- maximum deflection
σ_m- maximum stress
σ_y- yield stress
l_b- lap length
P_m- maximum loading

The overall performance of the beams with lap lengths can be characterized through the analysis of load-deflection curves. Figure 14 presents the load-displacement characteristics of the seven beams subjected to testing. Furthermore, Table 4 details the displacement measurements alongside the corresponding maximum load values. In general, the beam specimens exhibited satisfactory performance throughout the experimental procedure, indicating sufficient failure warning and ductility. However, the specimens with the shortest lap splice lengths (SS-30Ø and MS-30Ø), which had a lap splice length to diameter ratio ($l_b/Ø$) of 30, encountered abrupt failure attributed to bond failure.

It is important to recognize that the load analyzed in this study encompasses both the influence of the steel beam (0.98KN) positioned on the specimen and the corresponding bending moment induced by the self-weight of the tested reinforced concrete beam. During the transition from the uncracked to the cracked phase, a gradual and non-linear response was noted. Initially, multiple vertical cracks emerged within the constant moment region, followed by shear cracks near the support (see Figure 9-13). Figure 14 demonstrates that beams featuring lapped bars displayed varying degrees of ductility, marked by the formation of longitudinal splitting cracks along the lap splices. Conversely, the control beams with continuous bars exhibited ductile failure, characterized by vertical flexural cracking resulting from rebar yielding. Two distinct types of splice splitting failures were identified: (1) face splitting failure, characterized by vertical cracks forming beneath the lapped bars, and (2) side-splitting failure, where cracks appeared on the sides of the bars within the beam.

The research findings indicate that beams with extended lap lengths demonstrate increased rigidity in the early stages and exhibit enhanced resistance to peak stress prior to the reinforcement bars reaching their plastic threshold. Furthermore, the data illustrates a notable improvement in the ductility of the specimens as the lap length is increased. However, it is crucial to recognize that surpassing a lap length of 50 bar diameters of mild steel is impractical, as it interferes with the proper pouring and vibration of concrete. This interference can lead to the formation of air pockets, which may adversely affect the quality and performance of the structure. Additionally, while lap splicing is regarded as a simple method that does not necessitate specialized skills or tools, increasing the lap length of the reinforcing bars can lead to congestion and raise construction costs.

Figure 14 demonstrates that incorporating a lap length of 62Ø, as specified by Eurocode 2, significantly improved the stiffness, strength, and ductility of the specimen in comparison to the specimen lacking a lap length. This enhancement can be explained by the fact that the lap length of 744 mm encompasses 50% of the beam's total length, resulting in a cross-sectional area of the reinforcement bar that is double that of specimens without a lap length positioned in the beam's midsection. It is crucial to recognize that in practical applications, where the ratio of lap length to span length is minimal, the strength would approximate that of specimens without a lap length.

The results unequivocally indicate that the lap length specifications specified in EC2 provide adequate safety and ductility for mild steel. In contrast, after the onset of cracking, the stainless steel reinforced concrete beams displayed a more linear response than the mild steel specimens (MS-30Ø, MS-40Ø, MS-50Ø, and MS-62Ø).

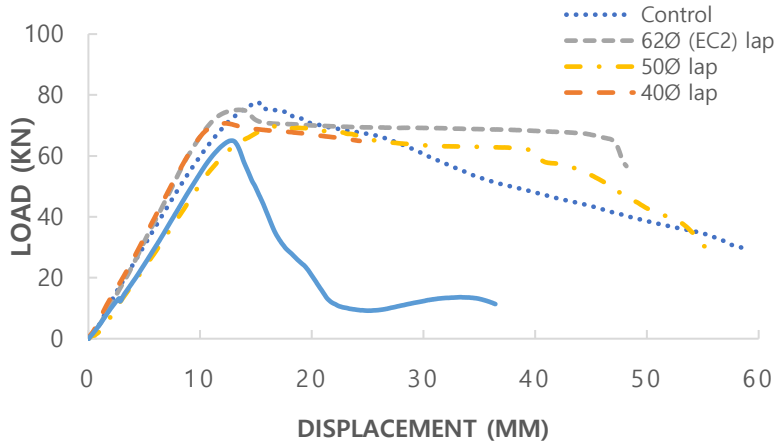

(a) Mild steel

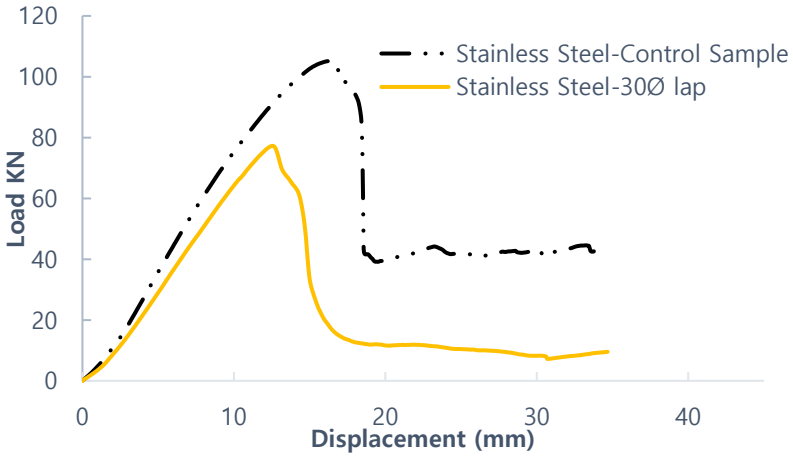

(b) Stainless steel

Fig. 14 Load-deflection relationship of specimens with various Sample lap length using mild an stainless steel

In examining the failure modes, beams reinforced with mild steel (MS-40Ø, MS-50Ø, and MS-62Ø) predominantly failed due to either bond failure or yielding of the reinforcement. Conversely, the stainless steel reinforced concrete beam, particularly the SS-00 specimen, failed as a result of concrete crushing. This difference can be explained by the superior stress-bearing capacity of stainless steel compared to mild steel, which allows it to withstand higher stress levels without experiencing plastic deformation. As a result, the strain in the top fiber of the concrete surpasses 0.003 before yielding occurs, leading to an abrupt failure. This phenomenon indicates that the area of steel reinforcement exceeds the balanced area of the steels. The results imply that to achieve the desired ductility, the steel area in the section should be less than that of mild steel, represented as $A_{s,ss} \leq \frac{f_{y,ms}}{f_{y,ss}} A_{s,ms}$ .Considering the stress-strain characteristics of stainless steels (as illustrated in Fig. 2), it can be inferred that specimens reinforced with stainless steel demonstrate enhanced ductility relative to those reinforced with mild steel. Thus, it is clear that, under equivalent beam specifications and loading conditions, stainless steel necessitates a reduced cross-sectional area, resulting in a more economical design. Furthermore, these findings underscore the necessity for the establishment of specific regulations regarding the strength and ductility of stainless steel, which should be advocated by the appropriate codes.

Figure 15 demonstrates that the beam reinforced with stainless steel (SS-30Ø) possesses a strength advantage over the beam reinforced with mild steel (MS-30Ø), with a difference of 19%. Furthermore, the ultimate strength ratio of the bars is recorded at 1.31, suggesting that the specimen failed prior to the bars achieving their ultimate strength. This phenomenon can be explained by the absence of a plastic phase in stainless steel, which leads to a higher internal bending moment and, as a result, enhanced strength. The control specimens exhibit a strength ratio of 1.35, consistent with the ultimate strength ratio of the bars. In contrast to the reinforced concrete beam utilizing stainless steel (SS-30Ø), the MS-30Ø beam shows marginally reduced initial stiffness and fails at an earlier point in time.

5. Conclusions

In this study, an experimental investigation was conducted to explore the potential for reducing the lap length in conventional reinforced concrete (RC) beams, with the

dual objectives of minimizing CO2 emissions and facilitating construction processes. The findings revealed that the lap length could be decreased by 20% in comparison to the design lap length specified in Eurocode 2 (62∅). This reduction not only promises a more cost-effective approach but also contributes significantly to the sustainability of RC frame structures, thereby contributing to a substantial decrease in CO2 emissions.

Additional technical results are presented as follows:

- The lap splices measuring 30 times the diameter (30∅), applicable to both mild and stainless steel, showed reduced failure loads in comparison to samples featuring longer lap lengths. These experimental results unequivocally indicate that the strength of a lap splice is directly related to its length.
- Three distinct failure modes were observed during the experiments. Lap splices measuring 30∅ experienced sudden bond failure prior to the yielding of the reinforcement. In contrast, lap splices of 40∅ failed subsequent to the yielding of the reinforcement, undergoing brittle bond failure following considerable plastic deflection. Conversely, lap splices with lengths of 50∅ and 62∅, as specified by Eurocode 2 for design lap lengths, demonstrated flexural failure. Thus, the transition from a lap length of 50∅ to 62∅ resulted in improved ductility, although it did not enhance strength. The performance of lap splices at 50∅ was found to be similar to that of the Eurocode 2 stipulated lap length of 62∅. Taking into account these results, along with considerations of project costs, sustainability, and the potential for reinforcement congestion linked to longer lap lengths, it can be inferred that the existing Eurocode 2 guidelines may not be sustainable.
- The overlapped regions of the specimens, specifically the 50∅ and 62∅ samples, demonstrated adequate ductility at their extremities, facilitating rotation and the formation of ultimate plastic hinges at the ends of the lap.
- Based on the conducted analysis, it was observed that increasing the lap splices beyond 50∅ does not provide any additional benefit in terms of strength.
- Furthermore, the specimens with stainless steel exhibited greater strength compared to those with mild steel, with a ratio of $\frac{f_{y,ss}}{f_{y,ms}}$
- To ensure the required ductility, for beams with the same properties, the area of stainless steel needs to be less than the area of mild steel by a factor of $\frac{f_{y,ss}}{f_{y,ms}}$
- The current regulations governing mild steel are not suitable for the design of structures utilizing stainless steel. Consequently, to ensure the required levels of ductility and strength, it is essential to establish separate regulations by implementing specific codes.
- The reduction in CO2 emissions is attributed to the shorter lap length.

6. References

Fib Bulletin (2013) fib Model Code for Concrete Structures 2010. Wiley. doi:10.1002/9783433604090.

BS EN 1992-1-1 (2004) “Eurocode 2: Design of concrete structures - Part 1-1 : General rules and rules for buildings,” British Standards Institution, 1(2004), p. 230. doi: [Authority: The Eur]opean Union Per Regulation 305/2011, Directive 98/34/EC, Directive 2004/18/EC].

CIBFIP (1991) CEB-FIP model code 1990: design code, Bulletin d’Information. London: Thomas Telford Services Ltd.

Fib Bulletin (2013) fib Model Code for Concrete Structures 2010, fib Model Code for Concrete Structures 2010. Wiley. doi:10.1002/9783433604090.

TG4.5, F. (2014) Bond and anchorage of embedded reinforcement: Background to the fib Model Code for Concrete Structures 2010.

Fib Bulletin 72 (2014) Bond and anchorage of embedded reinforcement: Background to the fib Model Code for Concrete Structures 2010. Lausanne, Switzerland.

Amin, R. (2009) End Anchorage at Simple Supports in Reinforced Concrete. London South Bank UniversitCairns, J. and

Eligehausen, R. (2014) “An evaluation of EC2 rules for design of tension lap joints’,” The Institution of Structural Engineers, p. 9.

Metelli, G., Cairns, J. and Plizzari, G. (2015) “The influence of percentage of bars lapped on performance of splices,” Materials and Structures/Materiaux et Constructions, 48(9), pp. 2983–2996. doi:10.1617/s11527-014-0371-y.

Cairns, J. (2014) “Staggered lap joints for tension reinforcement,” Structural Concrete, 15(1), pp. 45–54. doi:10.1002/suco.201300041

Cairns, J. (2013) “Lap splices of bars in bundles,” ACI Structural Journal, 110(2), pp. 183–191. doi:10.14359/51684399.

ACI committee 318 (2011) Building Code Requirements for Structural Concrete and Commentary (ACI 318M-11), American Concrete Institute, Farmington Hills, MI.

Uher, T. and Lawson, W., 1998. Sustainable development in construction. In: Proceedings CIB World Building Congress. Rotterdam, Netherlands: in-house publishing

Ortiz, O., Castells, F. and Sonnemann, G., 2009. Sustainability in the construction industry: A review of recent developments based on LCA. Construction and Building Materials, 23(1), pp.28-39.

Yılmaz, M. and Bakış, A., 2015. Sustainability in Construction Sector. Procedia - Social and Behavioral Sciences, 195, pp.2253-2262.

González, M. and García Navarro, J., 2006. Assessment of the decrease of CO2. emissions in the construction field through the selection of materials: Practical case study of three houses of low environmental impact. Building and Environment, 41 Malhotra, V., 2010. Global warming and role of supplementary cementing materials and superplasticisers in reducing greenhouse gas emissions from the manufacturing of Portland cement. International Journal of Structural Engineering, 1(2), p.116

ORANGUN, C.O., JIRSA, J.O. and Breen, J.E. (1977) “A Reevaulation of Test Data on Development Length and Splices,” ACI Journal Proceedings, 74(3), pp. 114–122

Tohidi M, Baniotopoulos C. (2017). Use of tie bars to prevent progressive collapse of precast cross wall structures, Engineering Structures 152, 274-288

Micallef, M. and Vollum, R.L. (2018) “The behaviour of long tension reinforcement laps,” Magazine of Concrete Research, 70(14), pp. 739–755. doi:10.1680/jmacr.17.00285.

Najafgholipour, M.A. et al. (2018) “The performance of lap splices in RC beams under inelastic reversed cyclic loading,” Structures, 15. doi:10.1016/j.istruc.2018.07.011.

Reynolds, G. and Beeby, A.W. (1982) “Bond in Concrete,” in Proceedings of the International Conference on Bond in Concrete. London: Applied Science Publishers, pp. 434–445.

jirsa, J. O., Chen, W., Grant, D.B.& E. (1995) Development of bundled reinforcing steel. Austin Texas.

Magnusson J (2000) Bond and anchorage of ribbed bars in high-strength concrete. Chalmers University, Go¨teborg, Sweden.

Ferguson, P. and Breen, J. (1965) "Lapped Splices for High Strength Reinforcing Bars," ACI Journal Proceedings [Preprint]. doi:10.14359/7738.

Chinn James Phil M., Ferguson Phil M. and Thompson J Neils. (1955) "Lapped Splices in Reinforced Concrete Beams," ACI Journal Proceedings, 52(10), pp. 201–213. doi:10.14359/11597

Rezansoff, T., Konkankar, U.S. and Fu, Y.C. (1992) "Bond Performance of Reinforcing Bars Embedded in High-Strength Concrete," Canadian Journal of Civil Engineering, 19, pp. 447–453.

Einea, A., Yehia, S. and Tadros, M.K. (1999) "Lap splices in confined concrete," Structural Journal, 86(6), pp. 947–955.

Shamass R, Cashell KA. (2019). Analysis of Stainless steel-concrete composite beams Journal of Constructional Steel Research, Elsevier

HJ Pam, JCM Ho. (2010). Effects of steel lap splice locations on strength and ductility of reinforced concrete columns. Advances in Structural Engineering

Widjaja Daniel, Darma1 Rachmawati, Titi Sari Nurul, Kwon, Keehoon1, Kim, Sunkuk (2023). Investigating Structural Stability and Constructability of Buildings Relative to the Lap Splice Position of Reinforcing Bars. Journal of The Korea Institute of Building Construction. Vol. 23, No. 3, pp. 315-326

Baddoo NR. (2008]. Stainless steel in construction: A review of research, applications, challenges and opportunities - Journal of constructional steel research, Elsevier

Gardner L.(2005). The use of stainless steel in structures. Progress in Structural Engineering and Materials, Wiley Online Librar

Rasmussen KJR. (20030. Full-range stress–strain curves for stainless steel alloys - Journal of constructional steel research, Elsevier

Gonzalez BM, Castro CSB, Buono VTL. (2003). The influence of copper addition on the formability of AISI 304 stainless steel … - Materials Science and …, Elsevier